Metals and Materials International
https://doi.org/10.1007/s12540-023-01396-9

Study on the Influence of Nickel Additions on AA7020 Formability Under Superplastic Forming Like Conditions

S. Taylor[1] · V. Janik[2] · R. Grimes[1] · R. Dashwood[2]

Received: 14 November 2022 / Accepted: 13 January 2023

Abstract
This study set out to look at the influence of nickel additions on a commercially available AA7020 to understand the impact of the resultant intermetallics on recrystallization, formability and material strength. Elevated temperature tensile testing across a range of strain rates (5×10^{-4} s^{-1} $\times$ 10^{-1} s^{-1}) and three temperatures (450– 500 °C) to compare material ductility followed by gas bulge testing at 475 °C and two gas pressures to investigate formability in a test closer to industrial forming conditions. Material strength was established using standard tensile testing, and EBSD used to understand the microstructural evolution of the materials. It was seen that the nickel additions increased ductility of the material across all test conditions, coupled with increasing the material strength. This was achieved due to the formation of nickel rich intermetallics which refine the microstructure during pre-heating through particle stimulated nucleation and subsequently improve strength through precipitation hardening in aging treatments.

Keywords Aluminium · Superplastic forming · Quick plastic forming · EBSD · Aluminium alloys

1 Introduction

Due to ever more stringent regulations to meet carbon emission reduction goals there is a need to make current internal combustion engine vehicles more efficient. This is being approached from two sides, improving the engine efficiency where we see the use of smaller displacement engines combined with turbochargers, and secondly by reducing the overall mass of the vehicle by moving to lightweight alloys and materials [1, 2]. There is also a significant rise in the development and uptake of electric vehicles, driven by regulations to ban the sale of new internal combustion engine vehicles from 2030 where there is the need for advanced lightweight materials to counteract the battery and motor mass which reduces vehicle efficiency and range [3–5].

The 7000 series alloys are high strength heat treatable alloys that offer a solution to the question of mass reduction in a wide range of industrial applications owing to their high strength the weight ratio [6, 7]. The ability to be warm or hot formed when combined with advanced forming processes such as superplastic forming (SPF), quick plastic forming (QPF) and hot form quench (HFQ), allows for complex geometries to be produced leading to a reduction in parts and joining processes [8]. The high strength of the materials allows for substitution of more dense materials such as steels or for downgauging of lower strength aluminium alloys, leading to a mass reduction in the produced parts [9].

The suitability of various 7000 series alloys in advanced forming operations to produce complex automotive parts has been widely demonstrated. The suitability of AA7050 to be hot or warm formed has been investigated, with processing maps identifying has been shown to offer optimal ductility around 420 °C and up to 0.18 s^{-1} indicating the potential for use in a QPF process [10]. Rong et al. demonstrated that within a Nakajima test to develop a thermal forming limit diagram AA7075 offered significantly improved ductility at 400 °C compared to 300 °C coupled with the ability to be formed at higher strain rates at higher temperature [11]. An alternative method to develop a similar thermal forming limit curve of AA7050 under HFQ forming conditions showed further improvements in formability at 450 °C [12]. AA7020 has been investigated in a variety of hot and warm forming applications and has been shown to demonstrate improved formability when combined with these processes

✉ S. Taylor
scott.taylor.1@warwick.ac.uk

[1] WMG, The University of Warwick, Coventry CV4 7AL, UK

[2] Coventry University, Priory St, Coventry CV1 5FB, UK

Published online: 11 February 2023

in the 150–250 °C range [[13]. Further details of the use of 7000 series alloys in elevated temperature processes can be found in reviews by Hirsch, Zheng and [7, 8 and 16]. Alternative methods of improving the formability of AA7075 have shown that it is possible to form an automotive b-pillar using w temper forming, where the material is solutionized and then later formed cold [17].

Previous investigations have reported that additions of nickel can lead to improvements in the formability of aluminium alloys with elongations of up to 800% reported in a 7000 series alloy [18]. The addition of nickel is reported to produce coarse intermetallic particles within the alloy, these particles have been shown to produce a finer grain structure during solutionization treatments prior to forming by means of particle stimulated nucleation (PSN) due to the high levels of local lattice misorientations around the particle following cold rolling [19, 20].

Superplastic forming processes are typified by forming at low strain rates 10^{-4} s^{-1}, 10^{-2} s^{-1} and at elevated temperatures typically greater than 80% of the materials melting temperature [21]. Superplastic materials typically have a high strain rate sensitivity coefficient (m value) which describes a materials ability to resist necking during forming, a typical metal would have an m value $0.2 \leq$ whereas a superplastic material would be ≥ 0.5 [21]. Typically for a material to be considered superplastic extensions of at least 200%–400% should be achievable within uniaxial tensile testing [22]. There is an academic shift championed by particular academics and universities to define superplasticity as a minimum of 400% linear elongation and an 'm' value greater than 0.5 [23], whereas industrially parts are typically designed with a maximum of 150% elongation [9].

This study set out to evaluate the formability of AA7020 under SPF and SPF like conditions to establish the optimum forming paraments for the alloy, and to evaluate whether it can be formed at higher strain rates to decrease forming times allowing it to be more widely adopted. Nickel containing variants of the same alloy were supplied by Norsk Hydro to understand whether the resulting intermetallics can offer any improvements in formability and strength. Elevated temperature tensile tests combined with elevated temperature gas bulge trials were utilized to establish formability whilst electron microscopy was employed to understand the microstructural evolution of the material at various stages of the process to inform industrial forming cycles.

2 Materials and Experimental Procedures

2.1 Materials

Two alloys were investigated in this study, a commercially available AA7020 alloy, and a nickel containing variant based on the original AA7020, named V3C within this report. Both alloys were supplied as 2 mm sheet in the cold rolled condition, no further thermomechanical processing as conducted prior to testing. The chemical composition of the two alloys is detailed in Table 1. Specimens for all tests were machined from sheet using a Datron CNC machine with a 3 mm cutter and optimized parameters to achieve a good surface finish along cuts.

2.2 Elevated Temperature Testing

Tensile dogbones with a gauge length of 20 mm as shown in Fig. 1a were machined in accordance with ISO 6892-2:2018 and tested using an Instron 5742 load frame with an integrated furnace [24]. Tests were controlled using Instron Wave Matrix V.2.35 software operating in strain rate control to achieve constant strain rates throughout testing. Tests were conducted across a range of strain rates ($5 \times 10^{-4}s^{-1}$, $1 \times 10^{-3}s^{-1}$, $5 \times 10^{-3}s^{-1}$, $1 \times 10^{-2}s^{-1}$, $5 \times 10^{-2}s^{-1}$, $1 \times 10^{-1}s^{-1}$) three temperatures (450 °C, 475°C, 500 °C) and with varied solutionization pre-heat times prior to deformation (1, 2 and 5 minutes). The furnace was allowed to stabilize at temperature for several hours prior to testing, samples were loaded into the grips with a 20N preload for the desired pre-heat time and then deformed to failure. Testing was conducted to investigate the influence of reducing pre-heat times and increasing strain rates to improve industrial forming processes and to assess influence of nickel containing intermetallics under the same conditions.

2.3 Gas Bulge Testing

250 mm square sets of material were prepared and lubricated in the region of the clamp ring with colloidal graphite acting as a release agent following testing, as the specimens were not in contact with the tooling during forming no further lubrication was required. Testing was conducted using an Interlaken forming press with a free bulge tool using a single central gas inlet at 475 °C and at two pressures (35Psi, 45Psi). Gas pressure and temperature was controlled using Interlaken Unitest software, all testing was conducted at a constant gas pressure as lack of feedback sensors would not allow for strain rate control of testing, failures were detected by a pressure drop in the system during forming. Dome heights were measured throughout testing using an integrated laser.

2.4 Tensile Testing

Tensile dogbones conforming to ISO 6892-1:2019 [25] were machined and then heat treated within a Nabotherm furnace to replicate the thermal cycles during testing but without any mechanical deformation. Following these heat treatments,

they were subjected to post forming aging treatments to assess the material strength following a typical industrial forming cycle. Specimens were the tested using an Instron 5567 load frame using Bluehill software with physical extensometers.

2.5 Microstructural Characterization

Microstructural analysis was conducted using Zeiss Sigma FEGSEM and an Oxford Instruments Nordlys EBSD camera with Oxford Aztec software. An aperture size of 240 µm and accelerating voltage of 20 keV was used across all scans, with a step size of 0.5 µm. Samples were prepared using a mechanical polishing regime modified from standard preparation techniques, with a final step of 1 h vibromet polishing wit colloidal silica to ensure a high-quality surface finish. Post processing of scans was conducted using Oxford Channel 5 software.

3 Results and Discussion

Flow curves for AA7020 and V3C across three temperatures are given in Figs. 2 and 3 respectively. Within the AA7020 we can see that the forming temperature did not significantly impact the elongation of the material, whilst having a marked influence on the peak stress being around 35 MPa at 450 °C and 25 MPa at 500 °C. At all three temperatures the material only experienced around a 0.1s difference in failure strain across the full range of strain rates investigated, with the material having an average 'm' value, of around 0.18 as shown in Fig. 2d. The 'm' value being the materials strain rate sensitivity which can be thought of as its resistance to localised necking, with higher resistance to localised necking being favourable for industrial forming. The 'm' value can be determined as the slope of a linear regression fit of by the log–log flow stress–strain rate plots at a certain strains, illustrated in Figs. 2 and 3 [26].The low 'm' value and limited ductility indicate the material is not capable of achieving SPF levels of ductility in an academic sense, and is less industrially relevant [27], the ability to reach near peak elongational higher strain rates does however indicate that the material may be suitable within a hot or warm forming application.

It was observed that the nickel containing variant V3C achieved greater strain to failure across all conditions, but with higher stress suggesting a stronger material as shown in Fig. 3a, b, and c. Unlike the AA7020 V3C showed a preference to deformation at higher temperatures with peak strains in excess of 1.0 s observed at both 475 and 500 °C. The V3C also exhibited a greater average 'm' value of 0.24 indicating a greater resistance to localized necking within the material. The greater levels of elongation in the V3C whilst still short of being strictly academically superplastic suggests more suitability within a wider range of industrial applications than AA7020. The presences of nickel rich intermetallics within the V3C is responsible for this increase in formability through increased static recrystallization kinetics due to PSN during pre-heating, and potentially through dynamic recrystallization during deformation. The maximum 'm' value of 0.26 is below the region where the stress exponent $n = 2$ which, as discussed by Sherby, indicates that grain boundary sliding is not an active deformation mechanism within either alloy. The low 'm' value and deformation at relatively higher strain rate would indicate the defor mation is mainly controlled by dislocation creep [27].

Both alloys showed close correlation of intermediate strain rates i.e.,1×10^{-2} s^{-1} and 5×10^{-3} s^{-1} and in the case V3C of notably improved ductility at higher temperatures. With this being the case, intermediate strain

Table 1 Chemical composition of alloys

Composition (wt%) Remainder Al										
Variant	Zn	Mg	Ni	Mn	Zr	Cr	Ti	Si	Fe	Cu
7020	4.5	1.6	0	0.22	0.1	0.2	0.02	0.05	0.1	0.002
V3C	4.57	1.25	1.61	0.22	0.101	0.2	0.022	0.05	0.098	0.002

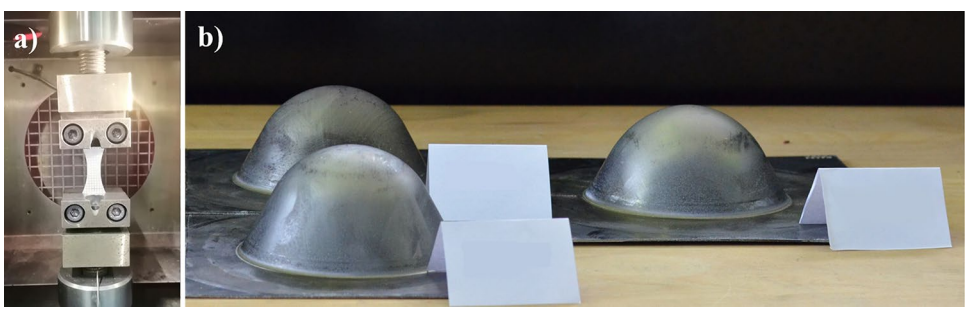

Fig. 1 **a** tensile dogbone prior to deformation within integrated load frame furnace, typical gas bulge specimens following failure

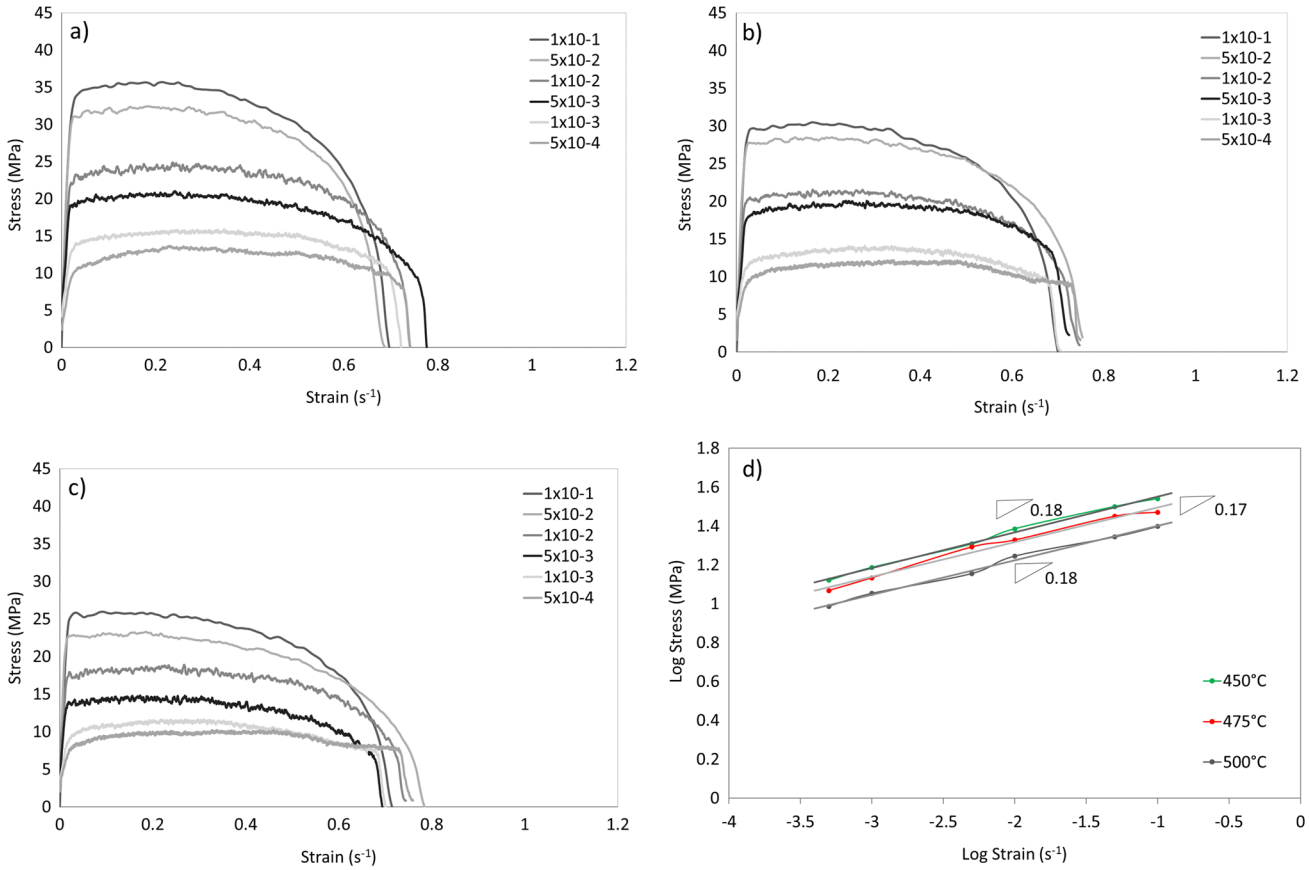

Fig. 2 Flow curves of AA7020 at **a** 450 °C, **b** 475 °C and **c** 500 °C, and **d** plot of 'm' value determination curve for all temperatures

rates and testing at 450 °C were removed from further testing to investigate the influence of preheat times on ductility to establish suitability for cycle time reductions within industrial forming processes. Typical hot forming processes utilize a five-minute preheat stage, this can represent a significant part of the overall forming cycle and is one of the limiting factors towards greater adoption of SPF like forming. Results of AA7020 exposed to varied pre-heat times at 475 and 500 °C are shown in Fig. 4a, b. respectively and for V3C in Fig. 5a, b. As previously the V3C was seen to outperform the AA7020 across all conditions, indicating increased formability due to the nickel additions.

Both alloys exhibited improved ductility when the preheat time was reduced from 5 minutes indicating that a 5 minute preheat leads to negative microstructural evolution such as grain growth. AA7020 achieved a peak linear elongation of 176% at 500 °C and $1 \times 10^{-2}\,s^{-1}$ with a two minute preheat and V3C achieved a peak elongation of 194% at 475 °C and $1 \times 10^{-1}\,s^{-1}$ with a two minute preheat. The increased ductility with a reduced preheat indicates a microstructural instability within the material at this time, indicating that static recrystallization not having fully completed and suggesting possible dynamic recrystallization during deformation. As would be expected for a material with lower strain rate sensitivity the AA7020 shows a "flatter" curve, indicating that it is less sensitive to the strain rate and more sensitive to the temperature at which it is formed as noted in other studies [28].

Previously the V3C had shown a preference to forming at 500 °C whereas with a reduced preheat time it proved to be more ductile at 475 °C. This indicates that the preheat time has a greater influence than the forming temperature, again linked to the presence of nickel intermetallics which are responsible for the improved ductility compared to the AA7020.

Free bulge testing was used to verify tensile results in an experiment closer to that found within an industrial forming process. Figure 6 shows the dome heights achieved for both materials at two different gas pressures to represent a fast and a slow strain rate. As with tensile results the V3C achieved a greater dome height than the AA7020 at both pressures, confirming that the V3C material has greater ductility than AA7020 across all investigated forming conditions. Again the V3C showed improved ductility at the higher gas pressure (higher strain rate), indicating its suitability towards

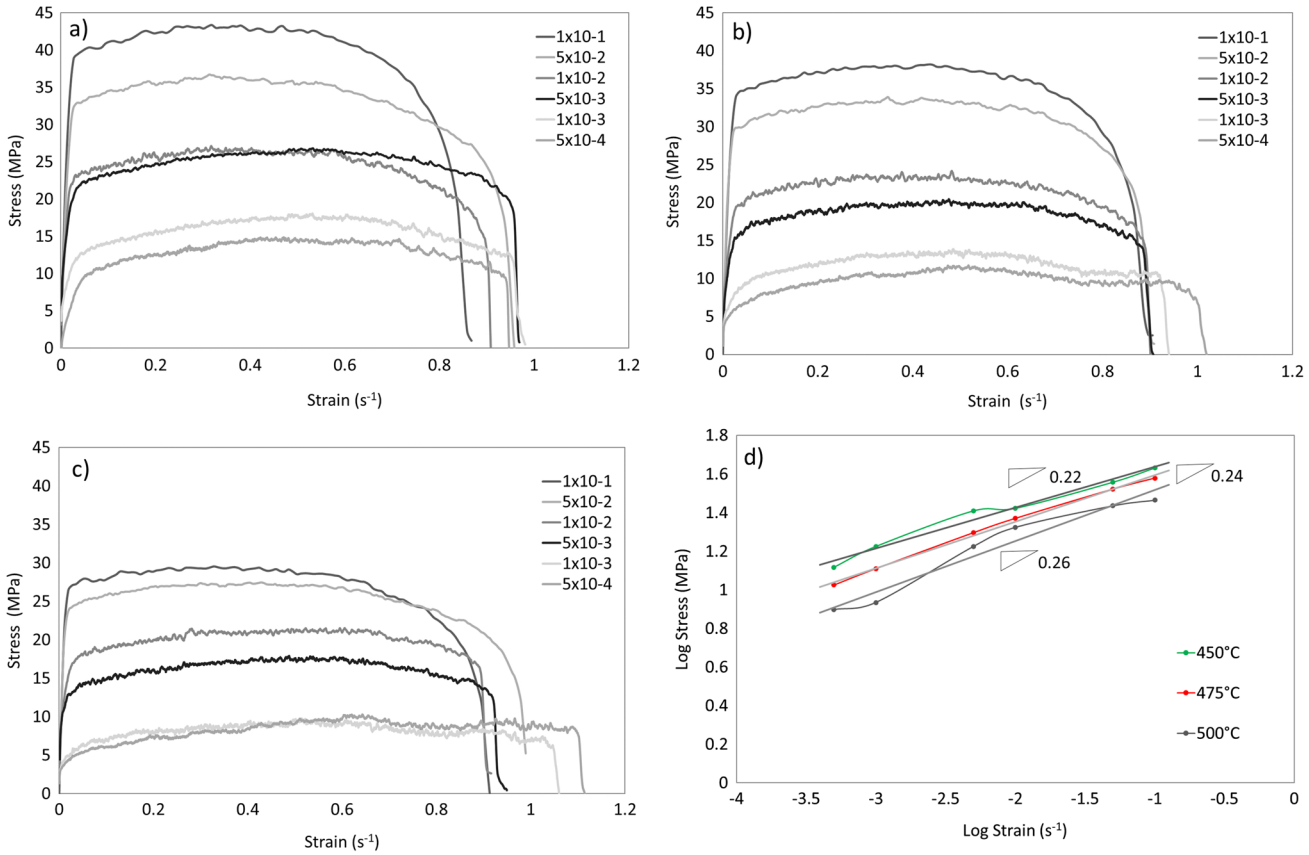

Fig. 3 Flow curves of V3C at **a** 450 °C, **b** 475 °C and **c** 500 °C, and **d** plot of 'm' value determination curve for all temperatures

industrial forming, and showing that the presence of nickel rich intermetallics positively impacts the ductility by influencing the microstructural evolution of the material both during preheat and whilst forming.

As seen in Fig. 7a, d. both materials exhibited a cold rolled structure in the as received condition, with clear bands of material running in the rolling direction. Figure 7 b, e. show AA7020 and V3C after heating to 475 °C but having experienced no deformation, both alloys show a structure with random orientation of grains which are reasonably equiaxed and with limited evidence of rolling direction, indicating fully recrystallized structures in both materials.

The main difference in the materials is the significantly finer grain structure observed within the V3C, this difference is due to the presence of nickel containing Al_3Ni particles which increase the influence of particle stimulated

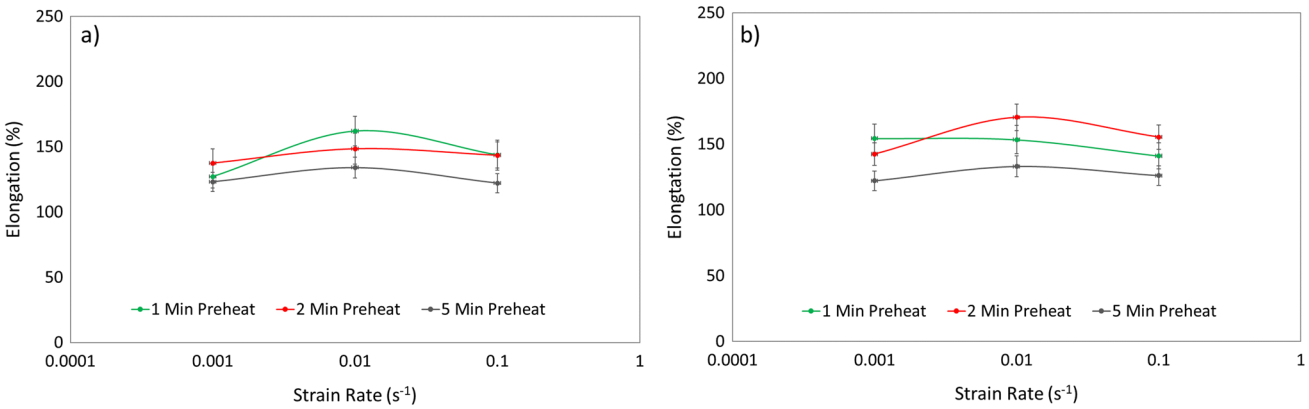

Fig. 4 Elongation versus strain rate with varied preheat times of AA7020 at **a** 475 °C and **b** 500 °C.

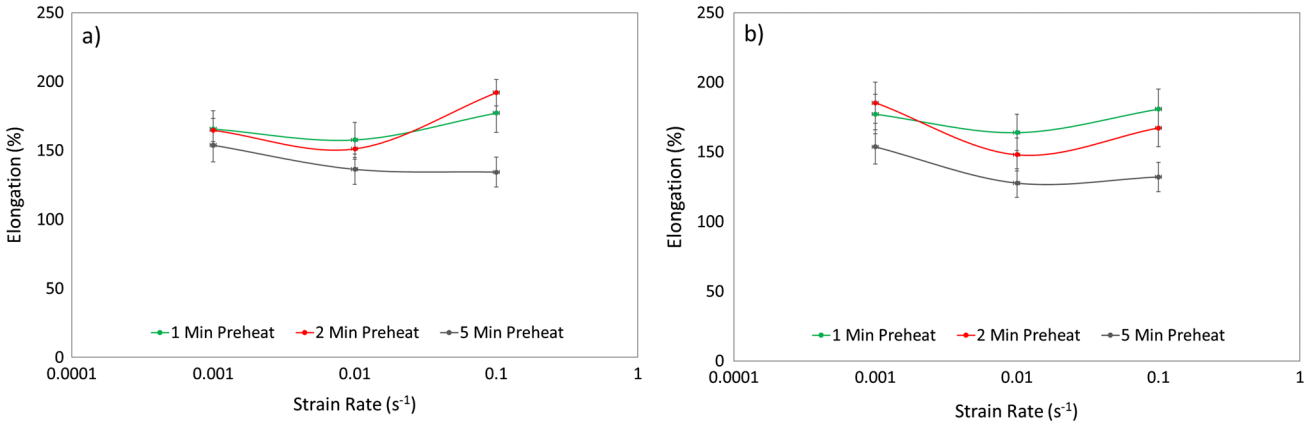

Fig. 5 Elongation versus strain rate with varied preheat times of V3C at **a** 475 °C and **b** 500 °C.

nucleation that leads to a finer recrystallized grain structure which has been demonstrated in various studies [18, 19, 29, 30]]. EDX analysis was used to confirm the presence of these particles within the V3C material, as shown in Fig. 7g these were well distributed throughout the as received cold rolled sample.

Figure 7c, f show the materials post forming, again there is a clearly finer grain structure within the V3C material compared to the AA7020. Within the V3C there is also more evidence of grain elongation and rotation towards the deformation direction suggesting some differences in deformation mechanisms within the two alloys owing to the nickel intermetallics. The main influence of the nickel addition and the subsequently formed nickel rich intermetallics being the increased recrystallization dynamics during static recrystallization through PSN and the subsequent finer grain structure which led to increased ductility of the alloy.

Both alloys were exposed to various aging treatments, and to a representative paint bake cycle as shown in Fig. 8a to investigate the influence of the nickel additions on material strength. As shown in Fig. 8b as with ductility, the V3C material was observed to outperform the AA7020 across all investigated aging treatments. Peak strength in both alloys was achieved using a combination of 90 °C for 8 hours and 180 °C for 18 h followed by the illustrated paint bake cycle. A peak yield strength of 320 MPa was observed in the AA7020 and 350 MPa in the V3C material. The cause of this is through increased precipitation hardening due to the presence of the nickel rich intermetallics which has been observed in other studies [31].

This study has demonstrated that the addition of Nickel to AA7020 is very beneficial in terms of mechanical properties, showing increases in ductility across all test parameters and improved strength across a range of heat treatments. This is achieved due to the formation of Al_3Ni particles and other nickel rich intermetallics which refine the microstructure

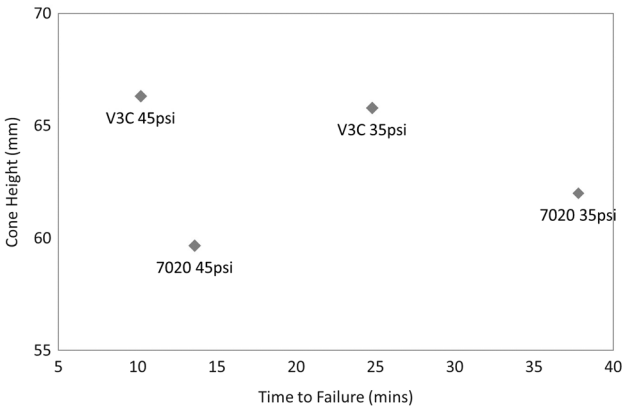

Fig. 6 Dome heights versus time to failure for both AA7020 and V3C at 475 °C for varied gas pressures

during pre-heating through PSN and subsequently through precipitation hardening in aging treatments. Further work is needed to identify how these intermetallics will impact the alloy in terms of joining and whether there is any detrimental impact on mechanisms such as stress corrosion cracking which is an issue for the wider uptake of 7000 series alloys.

4 Conclusions

From this study we draw several conclusions, the first being that a 1.6 wt% addition of nickel to AA7020 improves the material formability across all forming conditions regardless of strain rate or temperature. Under optimal conditions AA7020 achieved a linear elongation of 176% and V3C achieved 194%.

Neither alloy exhibits elongation which would be classically termed superplastic, however the study has demonstrated the ability to improve formability through the

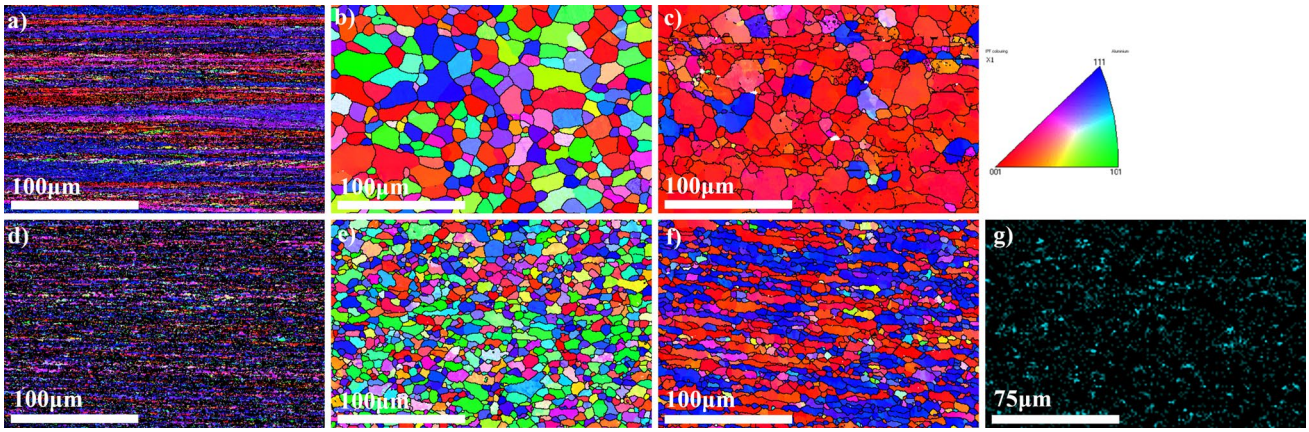

Fig. 7 IPF maps of AA7020 tensile dogbone, **a** as received, **b** non deformed region after deformation, **c** gauge length following deformation at $1 \times 10^{-2}\ s^{-1}$, V3C tensile dogbone, **d** as received, **e** non deformed region after deformation, **f** gauge length following deformation at $1 \times 10^{-2}\ s^{-1}$ and **g** EDX scan showing distribution of nickel intermetallics within V3C material

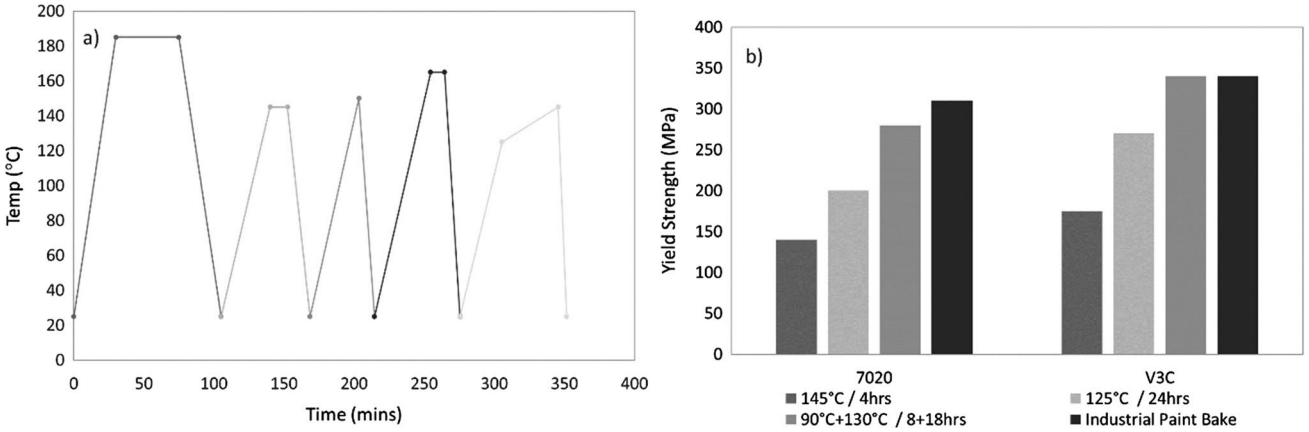

Fig. 8 **a** representative industrial paint bake cycle, **b** yield strength of AA7020 and V3C following various aging treatments

addition of nickel. This led to industrially relevant levels of elongation, particularly at higher strain rates with shorter preheat times, indicating the ability to reduce overall cycle times.

As with ductility, the addition of nickel had a positive impact on the strength of the material across all tested heated treatments. Peak strength in the base AA7020 was 320 MPa, increasing to 350 MPa for the V3C.

The formation of nickel rich intermetallics due to the added nickel was responsible for the increases in ductility and strength due to several mechanisms. Particle stimulated nucleation during preheating lead to a finer grain structure leading to improved ductility, and increased precipitation strengthening during aging treatments increased the material strength.

Acknowledgements The authors would like to acknowledge EPSRC for funding of this project, and Superform for both funding and research support during the project. The authors would also like to thank Norsk Hydro for material supply and in particular Simon Miller Jupp for instigating the investigation of nickel additions. In addition to that, the characterisation facility is supported from the Higher Education Funding Council for England (HEFCE) fund and the WMG Centre High Value Manufacturing Catapult is gratefully acknowledged.

Data Availability The raw/processed data required to reproduce these findings cannot be shared at this time due to technical or time limitations.

Declarations

Conflict of interest On behalf of all authors, the corresponding author states that there is no conflict of interest.

References

1. N. Hooftman, M. Messagie, J. Van Mierlo, T. Coosemans, Renew. Sustain. Energy Rev. **86**, 1 (2018)
2. S.H. Park, C.S. Lee, Prog. Energy Combust. Sci. **39**, 147 (2013)
3. J. Dernotte, P.M. Najt, R.P. Durrett, SAE Int. J. Adv. Curr. Pract. Mobility **2**, 2665 (2020)
4. F. Leach, G. Kalghatgi, R. Stone, P. Miles, Transp. Eng. **1**, 10005 (2020)
5. P.K. Senecal, F. Leach, Results Eng. **4**, 100060 (2019)
6. P.A. Rometsch, Y. Zhang, S. Knight, Trans. Nonferrous Met. Soc. China **24**, 2003 (2014)
7. J. Hirsch, Trans. Nonferrous Met. Soc. China **24**, 1995 (2014)
8. K. Zheng, D.J. Politis, L. Wang, J. Lin, Int. J. Lightweight Mater. Manuf. **1**, 55 (2018)
9. D. Edwards, Global automotive lightweight materials detroit 2016, https://www.galmintelligence.com/c547/global-automotive-lightweight-materials-detroit-2016/. Accessed 19 July 2022
10. S. Wang, L.G. Hou, J.R. Luo, J.S. Zhang, L.Z. Zhuang, J. Mater. Process. Techn. **225**, 110 (2015)
11. H. Rong, P. Hu, L. Ying, W. Hou, J. Zhang, Int. J. Mech. Sci. **156**, 59 (2019)
12. L.Y. Wang, W. Huang, H.C. Gheng, Y. Zhang, Investigation on forming limit diagram of 7075 aluminum alloy sheets under HFQ conditions, in *Proceedings of the Advanced High Strength Steel and Press Hardening, Proceedings of the 5th International Conference (ICHSU2020)*, Shanghai, 17–18 November 2020
13. M. Kumar, C. Poletti, H.P. Degischer, Mater. Sci. Eng. A **561**, 362 (2013)
14. M. Kumar, N. Sotirov, C.M. Chimani, J. Mater. Process. Technol. **214**, 1769 (2014)
15. J. Noder, R. George, C. Butcher, M.J. Worswick, J. Mater. Process. Technol. **293**, 117066 (2021)
16. B.A. Behrens, S. Hübner, H. Vogt, IOP Conf. Ser. Mater. Sci. Eng. **418**, 012027 (2018)
17. J. Lee, H.J. Bong, D. Kim, Y.S. Lee, Y. Choi, M.G. Lee, JOM **71**, 4393 (2019)
18. A.V. Mikhaylovskaya, A.D. Kotov, A.V. Pozdniakov, V.K. Portnoy, J. Alloys Compd. **599**, 139 (2014)
19. A.V. Mikhaylovskaya, V.K. Portnoy, Materialwiss. Werkst. **43**, 772 (2012)
20. F.J. Humphreys, Acta Metall. **25**, 1323 (1977)
21. G. Bernhart, P. Lours, T. Cutard, V. Velay, F. Nazaret, in *Superplastic Forming of Advanced Metallic Materials*, ed. by G. Bernhart (Woodhead Publishing, Sawston, 2011), pp. 49–71
22. T.G. Langdon, J. Mater. Sci. **44**, 5998 (2009)
23. M. Kawasaki, R.B. Figueiredo, T.G. Langdon, Adv. Eng. Mater **18**, 127 (2016)
24. ISO 6892-2:2018, Metallic materials — Tensile testing — Part 2: Method of test at elevated temperature (ISO, Geneva, 2018)
25. ISO 6892-1:2019, Metallic materials — Tensile testing — Part 1: Method of test at room temperature (ISO, Geneva, 2019)
26. T. Suo, Y. Chen, Y. Li, C. Wang, X. Fan, Mater. Sci. Eng. A **560**, 545 (2013)
27. O.D. Sherby, J. Wadsworth, Prog. Mater. Sci. **33**, 169 (1989)
28. R. Shabadi, S. Suwas, S. Kumar, H.J. Roven, E.S. Dwarkadasa, Mater. Sci. Eng. A **558**, 439 (2012)
29. S. Taylor, V. Janik, R. Grimes, R. Dashwood, Materialwiss. Werkst. **48**, 876 (2017)
30. A.V. Mikhaylovskaya, M.A. Ryazantseva, V.K. Portnoy, Mater. Sci. Eng. A **528**, 7306 (2011)
31. Y. Fan, K. Huang, M.M. Makhlouf, Metall. Mater. Trans. A **46**, 5830 (2015)